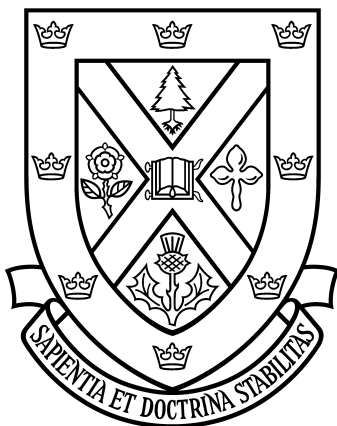


Superradiant Searches for Dark Photons in Two Stage Atomic Transitions



Joseph Bramante
Queen's University
McDonald Institute
Perimeter Institute

PI

Amit Bhoonah, **JB**, Ningqiang Song 1909.07387

Dark photons

$$\mathcal{L} = \mathcal{L}_{SM} - \frac{1}{4} F_{\mu\nu} F^{\mu\nu} - \frac{1}{4} F'_{\mu\nu} F'^{\mu\nu} + m^2 A'_\mu A'^\mu - (A_\mu + \chi A'_\mu) J_{EM}^\mu$$



Galison, Manohar 1984
Holdom 1986

U(1) vectors mixed with the SM photon appear in many SM extensions

SUSY breaking sectors

Dienes Kolda March-Russell 1998

String compactifications

Goodsell Jaeckel Redondo Ringwald 2008

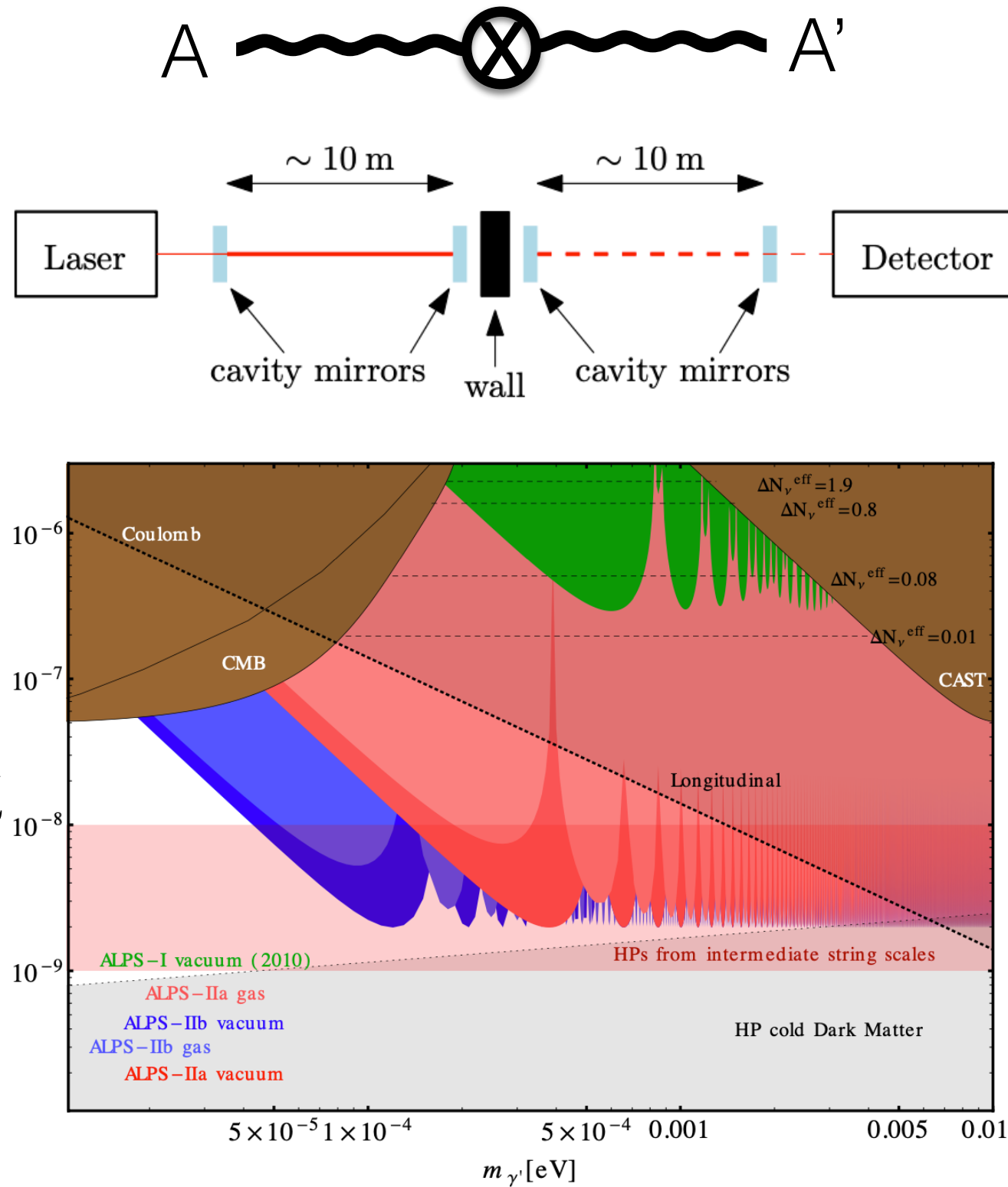
Dark sectors

Pospelov 2008

Arkani-Hamed Finkbeiner Slatyer Weiner 2008

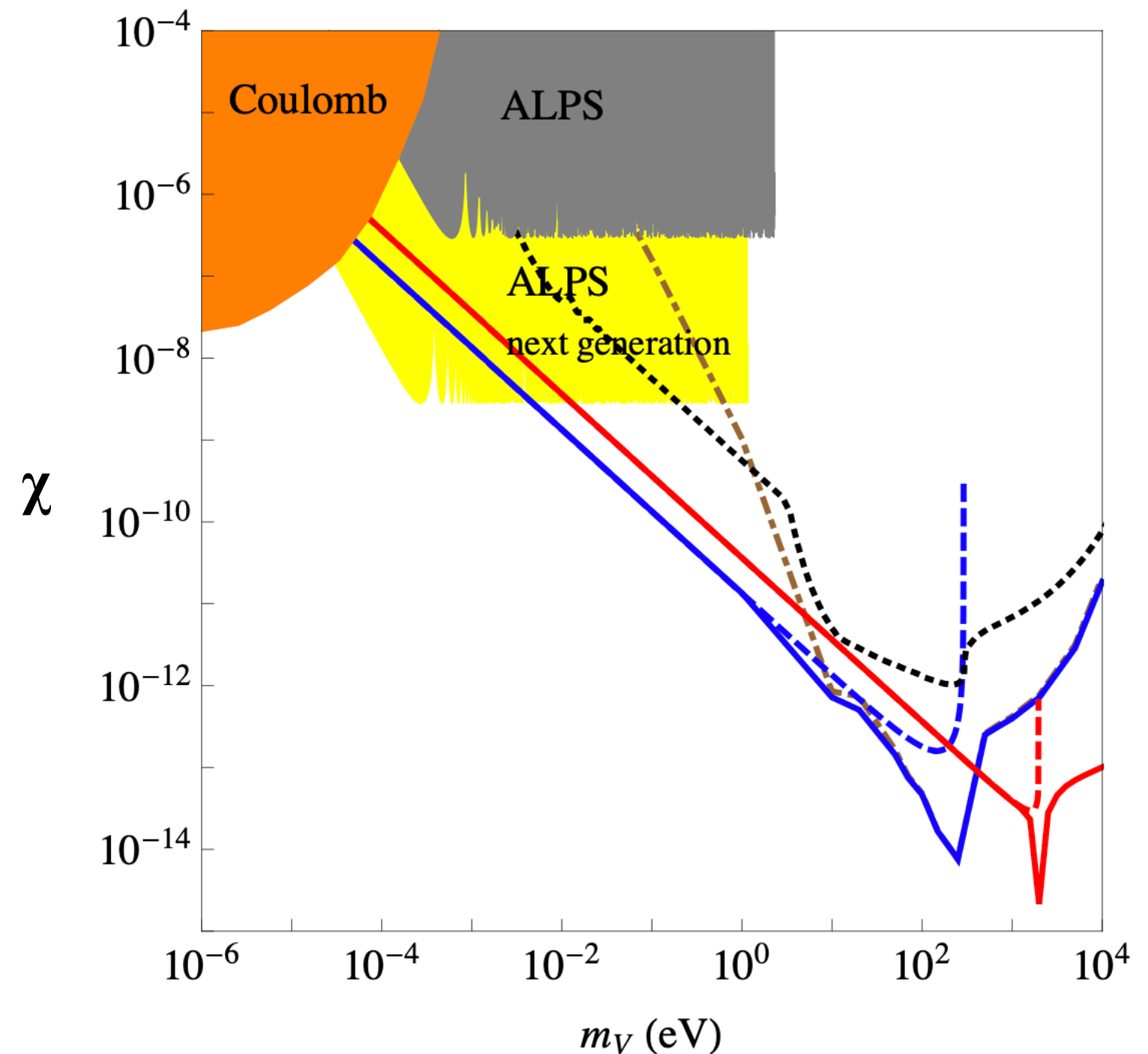
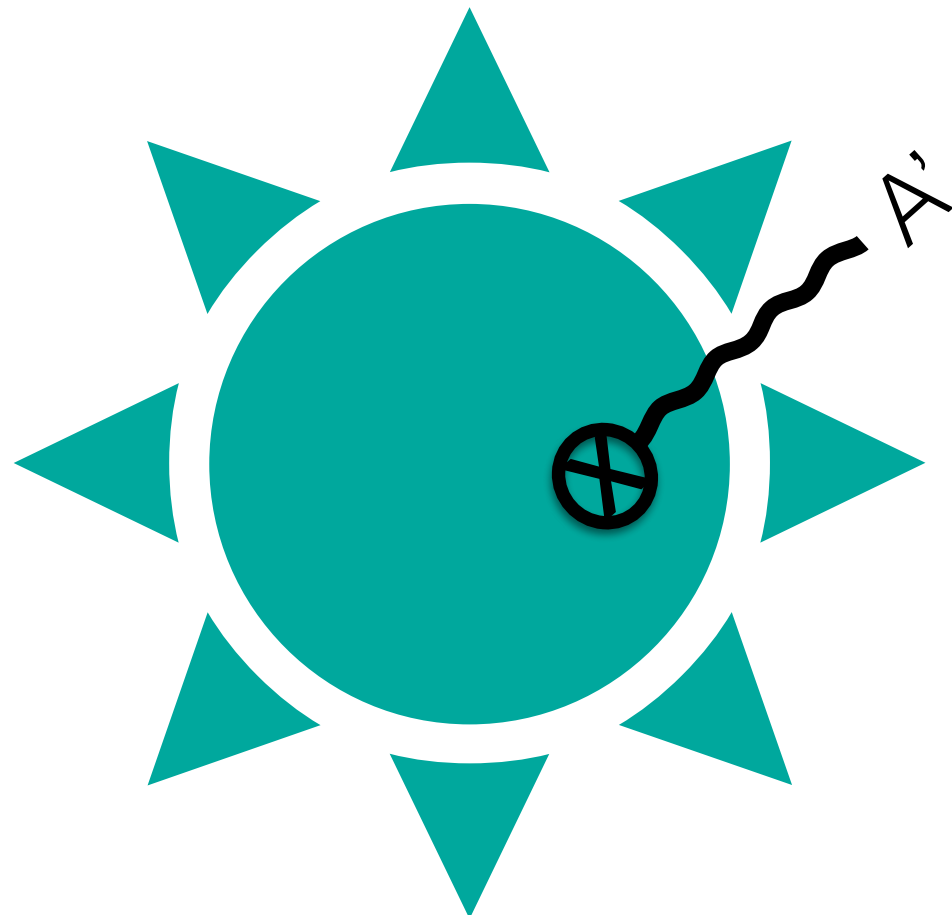
Ackerman Buckley Carroll Kamionkowski 2008

Light Shining Through Walls



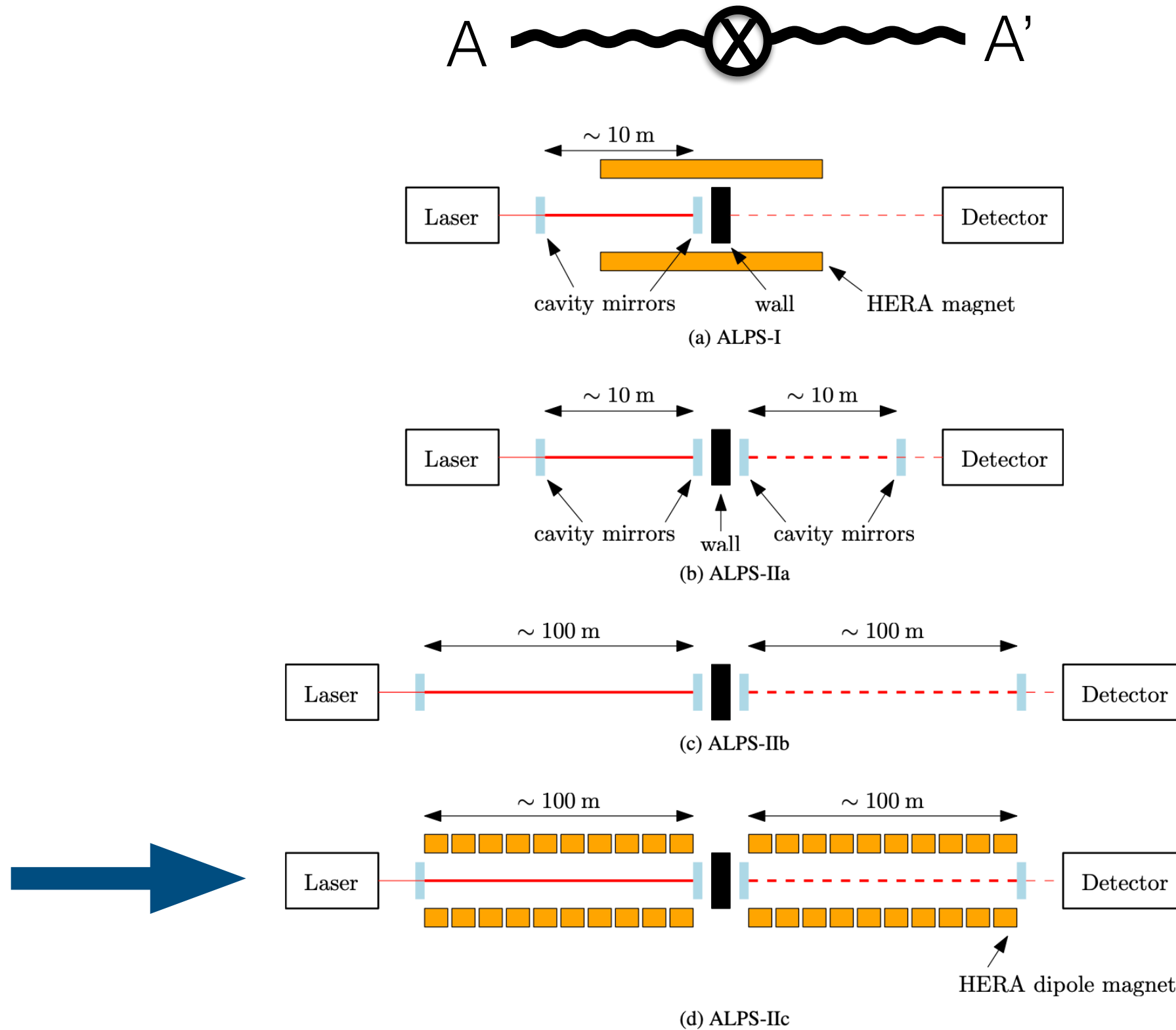
Searches for dark photons currently use cavities to detect the dark photons coming through the wall, (ALPS II).

Stellar emission with longitudinal mode



Stellar emission bounds currently leading for \sim meV+.

Light Shining Through Walls



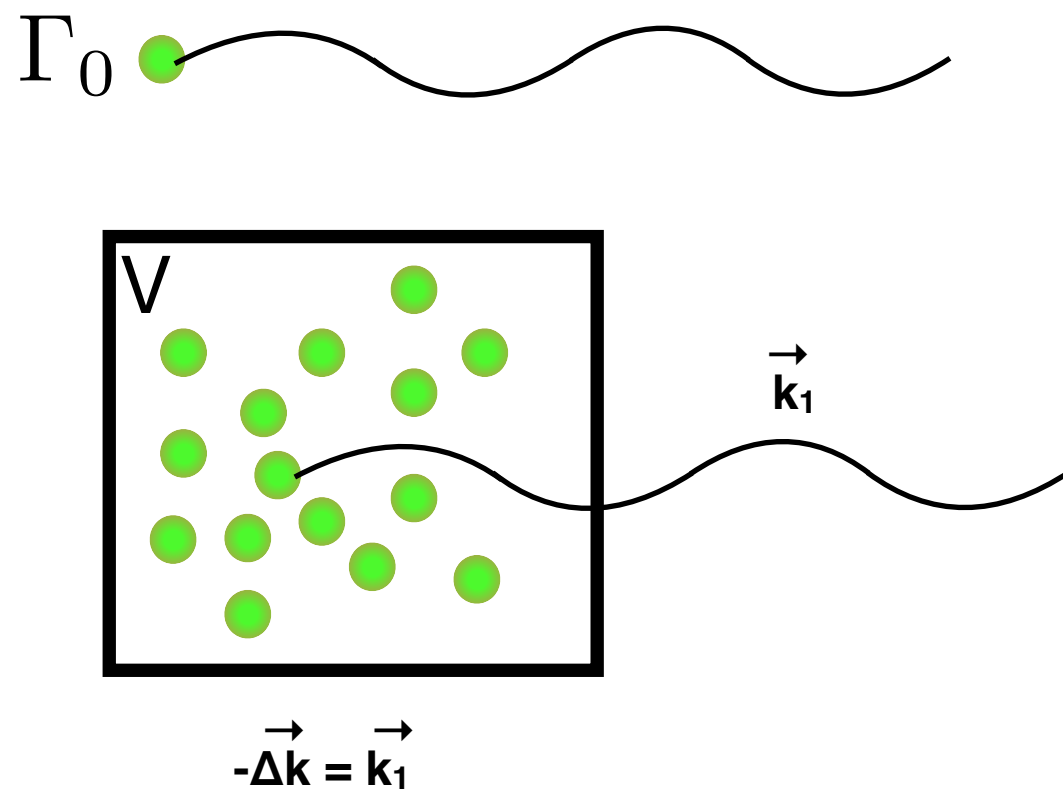
ALPS II focusing on axion detection.

ALPS II TDR 1302.5647

Classic Superradiance

Dicke 1954

Superradiance describes the collective (de-)excitation of atoms that emit or absorb photons coherently.



$$\Delta k \Delta x \sim 1$$

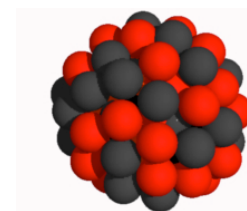
$$V \sim \frac{1}{k_1^3}$$
 coherence volume
momentum limited

$$\Gamma = nV\Gamma_0 \quad \text{No SR}$$

$$\Gamma_{tot} = n^2 V^2 \Gamma_0 \quad \text{SR}$$

Analogy to Spin-Independent Direct Detection: sum over emitters versus sum over nucleons in amplitude, squared.

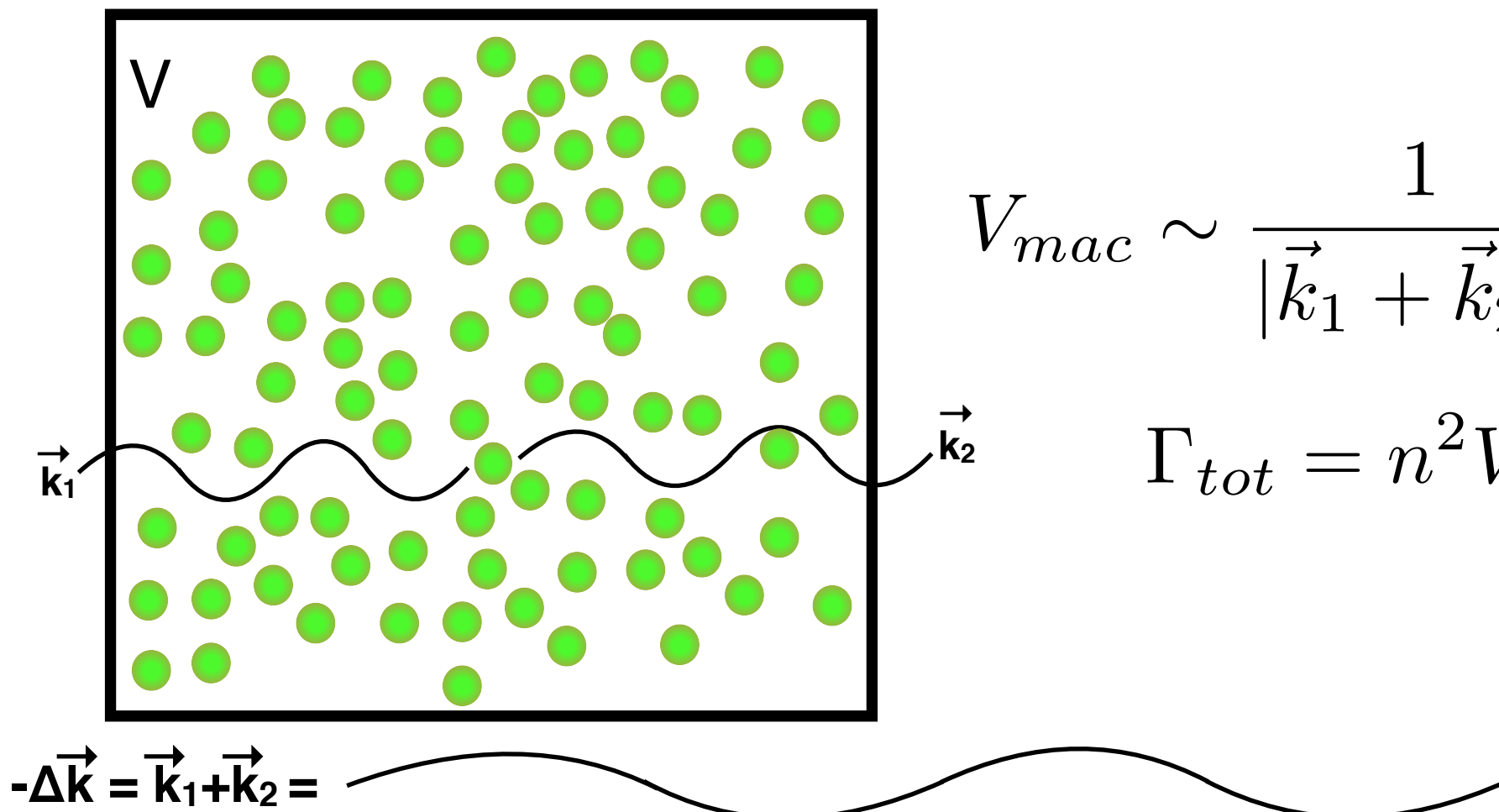
$$\sigma \propto N^2 \sigma_n$$



Macro Superradiance

Yoshimura 2006

Classic superradiance is limited by the frequency of the photon emitted. Macro superradiance minimizes the momenta of emitters with back-to-back two photon emission.



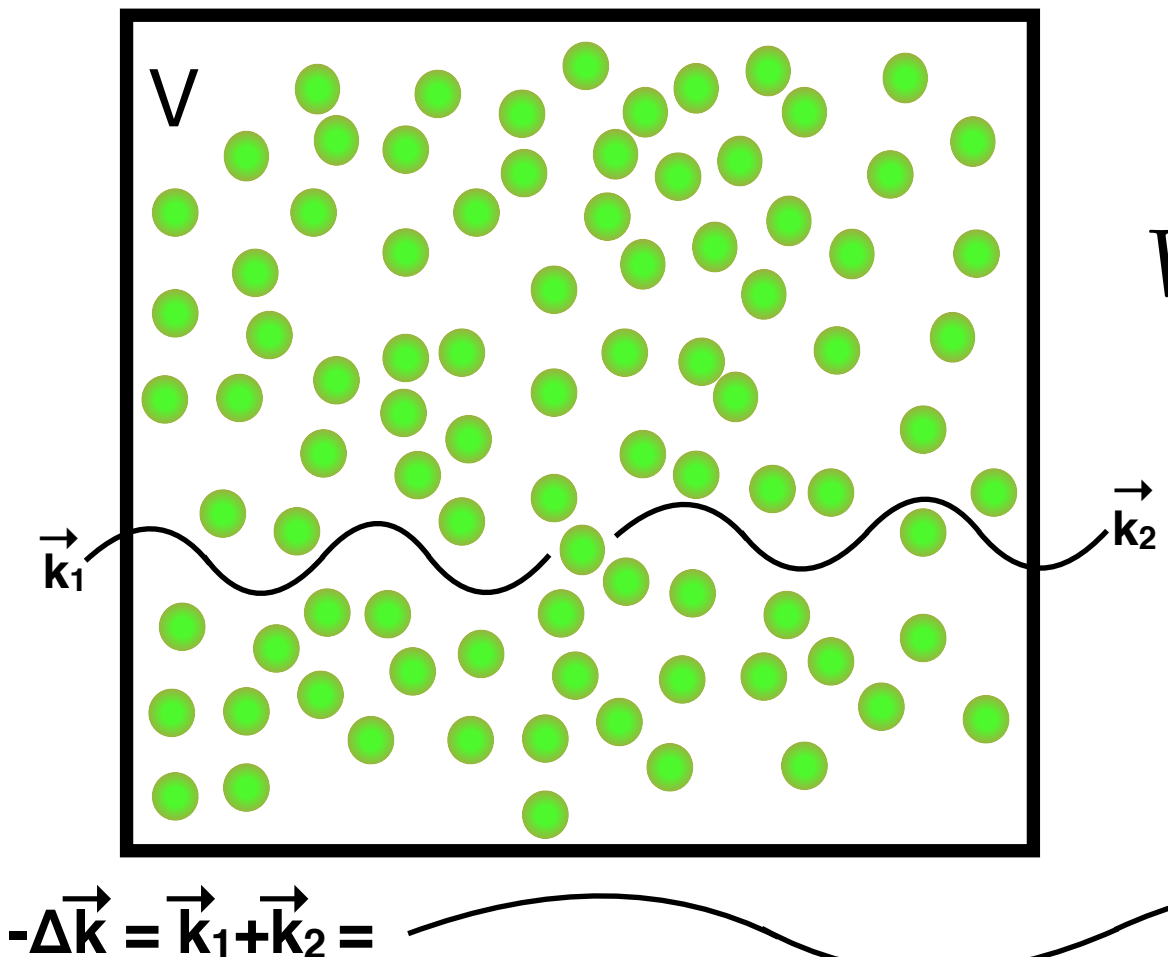
$$V_{mac} \sim \frac{1}{|\vec{k}_1 + \vec{k}_2|^3}$$
 macro coherence volume

$$\Gamma_{tot} = n^2 V_{mac}^2 \Gamma_0$$
 macro SR

Macro Superradiance

Yoshimura 2006

Classic superradiance is limited by the frequency of the photon emitted. Macro superradiance minimizes the momenta of emitters with back-to-back two photon emission.



$$V_{mac} \sim \frac{1}{|\vec{k}_1 + \vec{k}_2|^3} \quad \text{macro coherence volume}$$

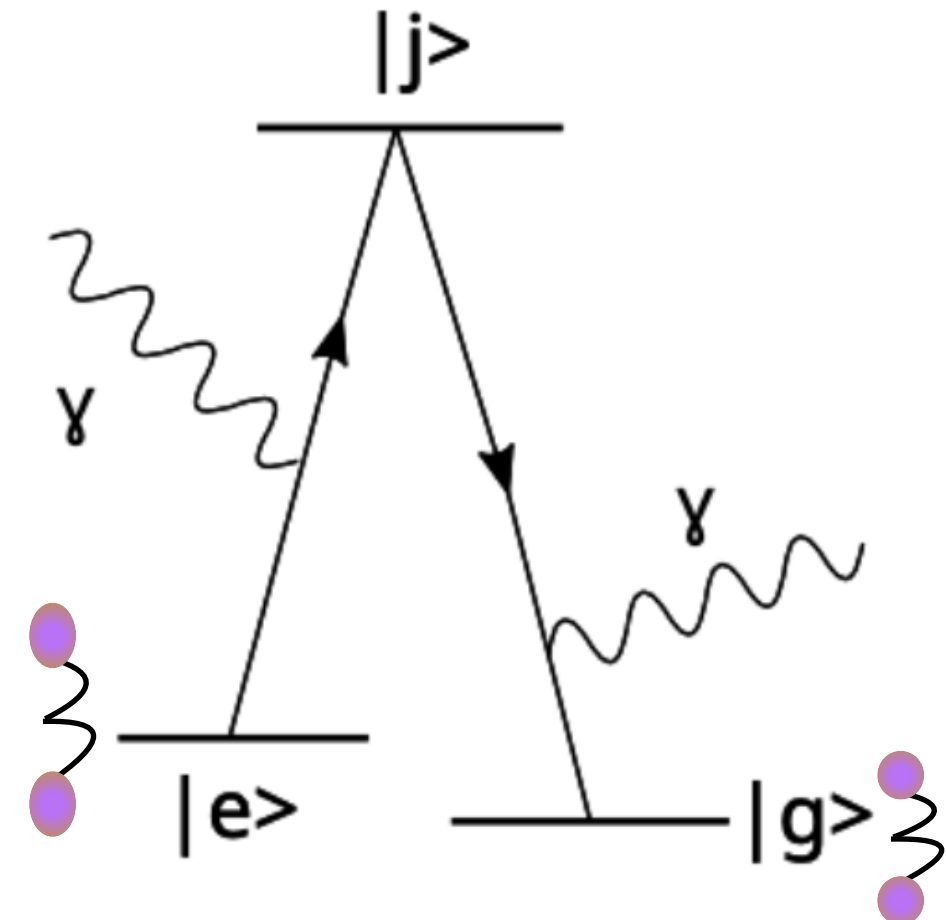
$$\Gamma_{tot} = n^2 V_{mac}^2 \Gamma_0 \quad \text{macro SR}$$

$$\Gamma_{sp} = \int \frac{d^3 k_1}{(2\pi)^3} \frac{d^3 k_2}{(2\pi)^3} \left| \int d^3 r \sum_{a=1}^N \frac{a_{eg}}{4} \sqrt{\frac{4\omega_1\omega_2}{V^2}} e^{-i(\vec{k}_1 + \vec{k}_2 - \vec{k}_{eg}^a)(\vec{r} - \vec{r}_a)} \right|^2 2\pi\delta(\omega_{eg} - \omega_1 - \omega_2),$$

Macro-coherent when phase difference minimized, $|\vec{k}_{eg}^a| \ll |\vec{r} - \vec{r}_a|$.

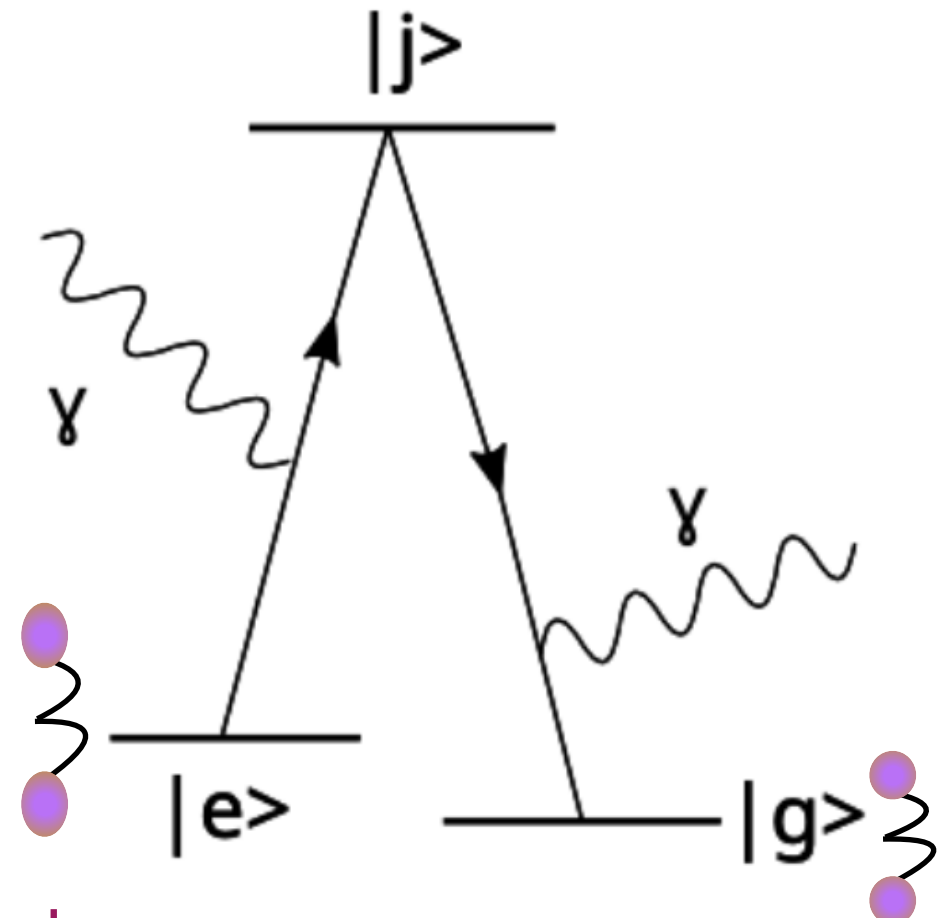
Macro Coherence in Parahydrogen

pH₂'s first vibrational excitation state electric dipole (E1) transition parity forbidden, leading transition is two photon (E1xE1).

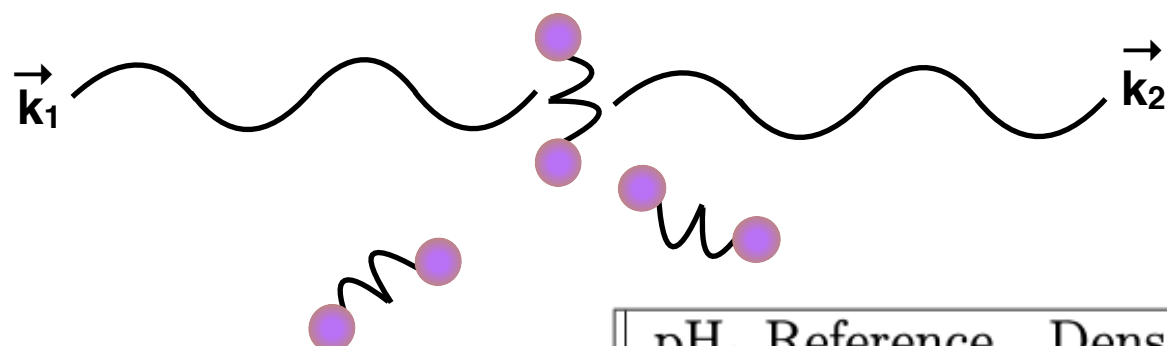


Macro Coherence in Parahydrogen

pH₂'s first vibrational excitation state electric dipole (E1) transition parity forbidden, leading transition is two photon (E1xE1).



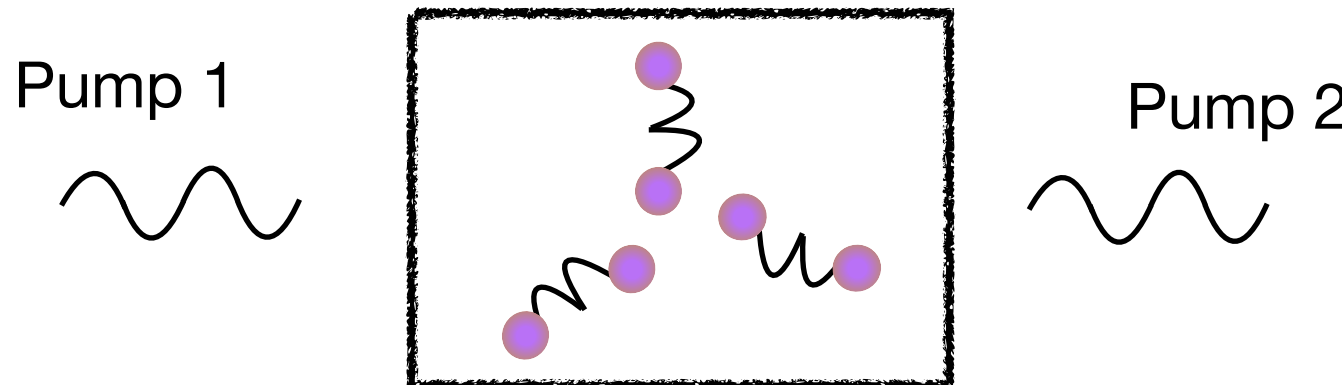
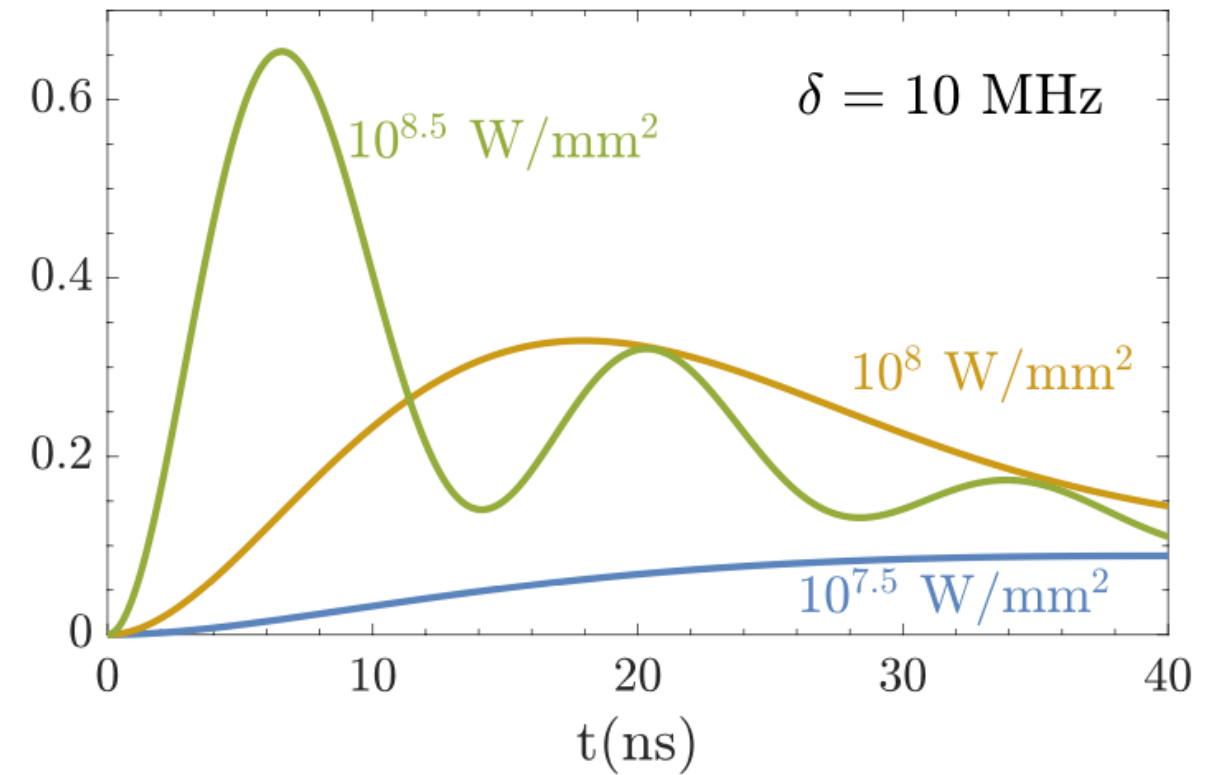
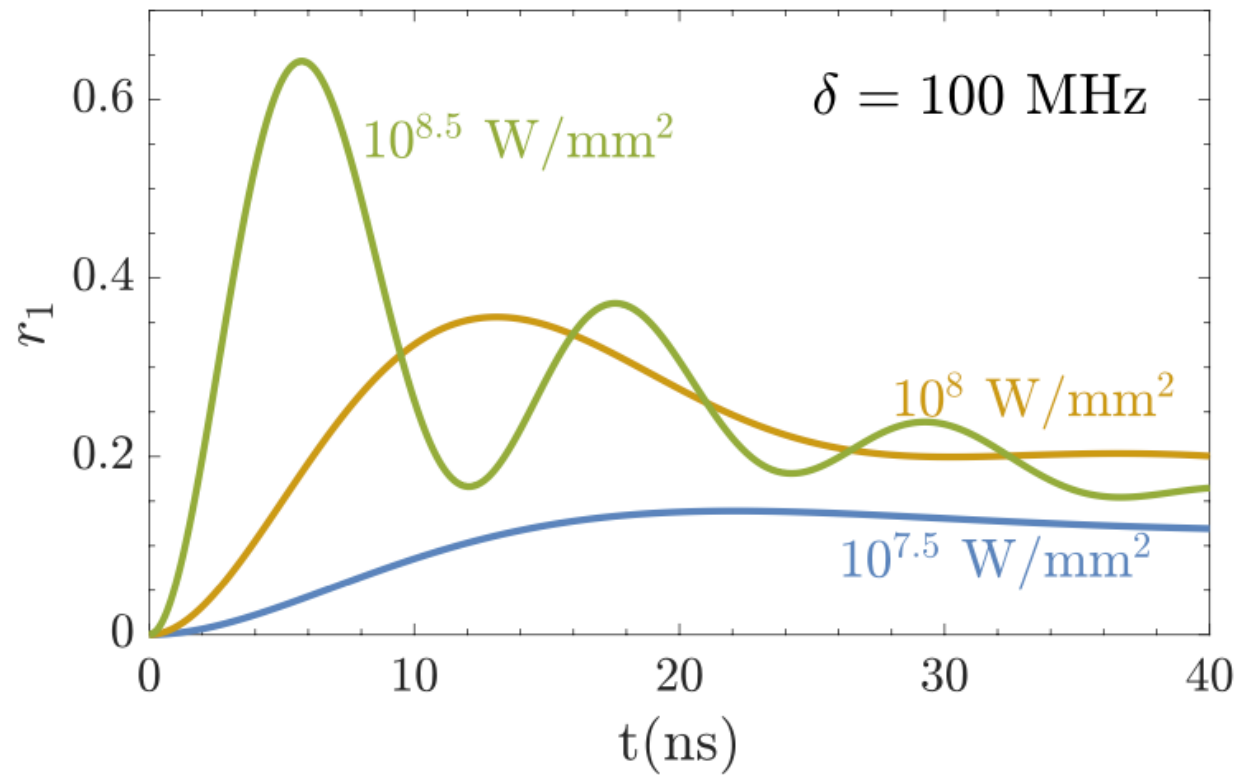
This ~0.5 eV vibrational mode is the lowest lying state, along with easily attainable 10 ns decoherence times, this makes pH₂ a good medium for macro coherence.



pH ₂ Reference	Density (cm ⁻³)	Temperature (K)	Decoherence Time (ns)
[57]	$10^{19} - 10^{20}$	80-500	~ 10
[42]	5.6×10^{19}	78	~ 8 (est)
[37]	$10^{19} - 5 \times 10^{20}$	78	~ 10 (est)
[58]	2.6×10^{22}	4.2	$\gtrsim 140$

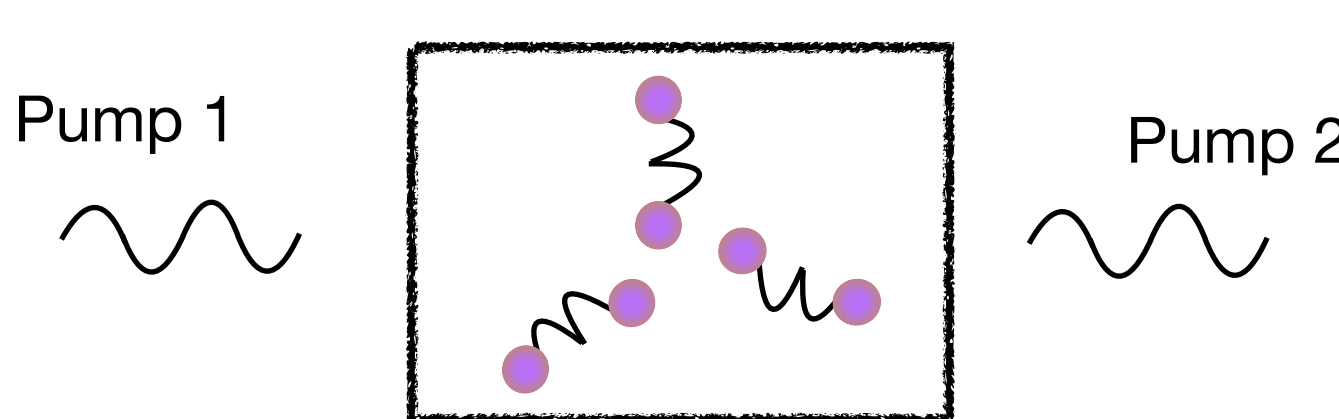
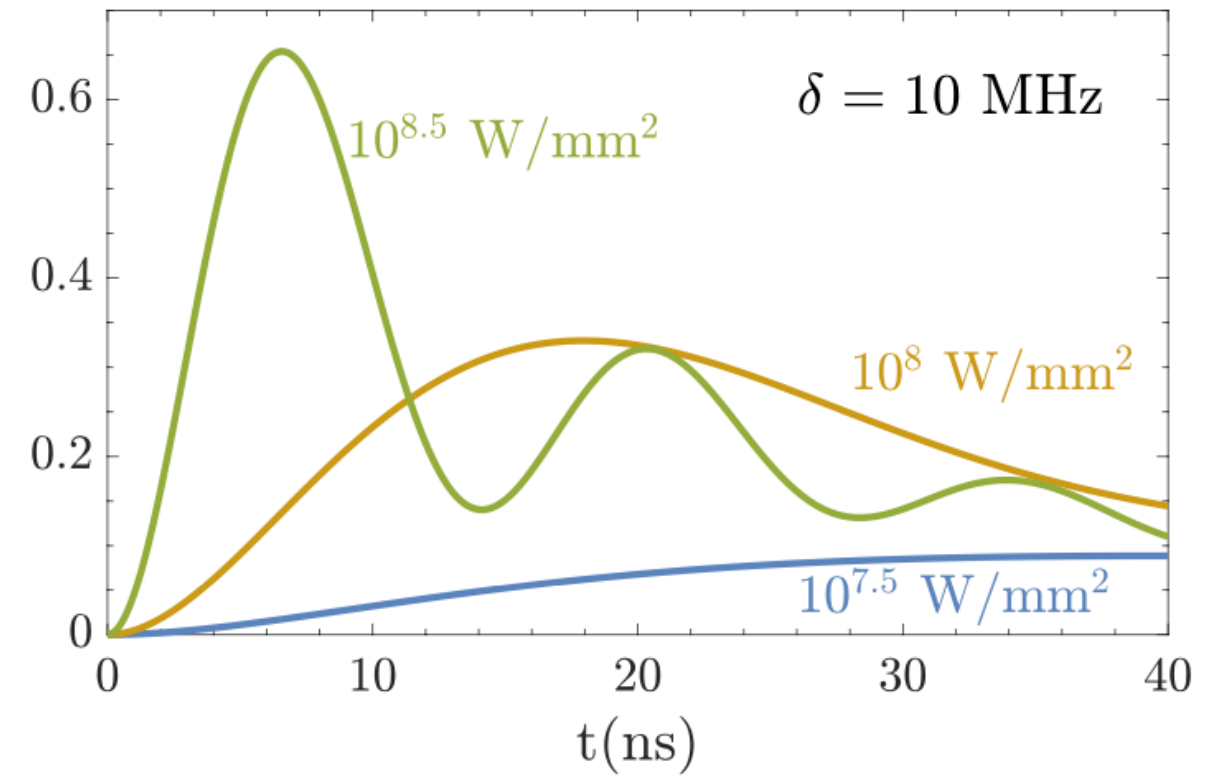
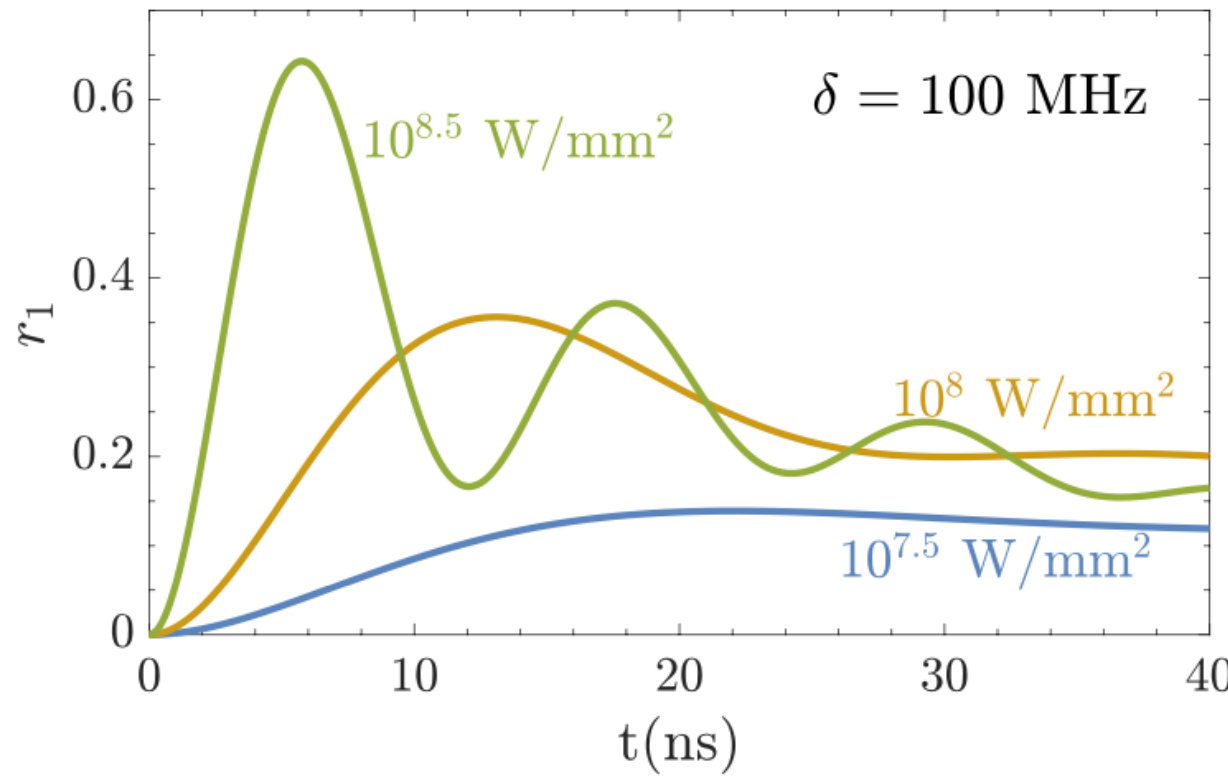
Macro Coherence in Parahydrogen

r_1 is the $|e\rangle, |g\rangle$ Bloch vector where $r_1 = 1$ defines fully coherent/in-phase atoms. Our simulations assumed 10 ns decoherence times, and varied laser detuning δ .



Macro Coherence in Parahydrogen

r_1 is the $|e\rangle, |g\rangle$ Bloch vector where $r_1 = 1$ defines fully coherent/in-phase atoms. Our simulations assumed 10 ns decoherence times, and varied laser detuning δ .

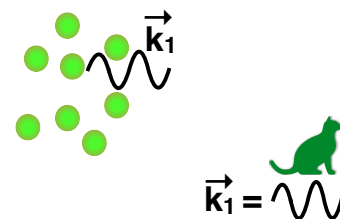


Superradiant Parahydrogen Target
Sample Length $L = 30$ cm
pH ₂ Density $n = 10^{21}$ cm ⁻³
Pump Laser Freq. $\omega_1 = 0.26$ eV
Pump Laser Power $\approx 10^9$ W mm ⁻²

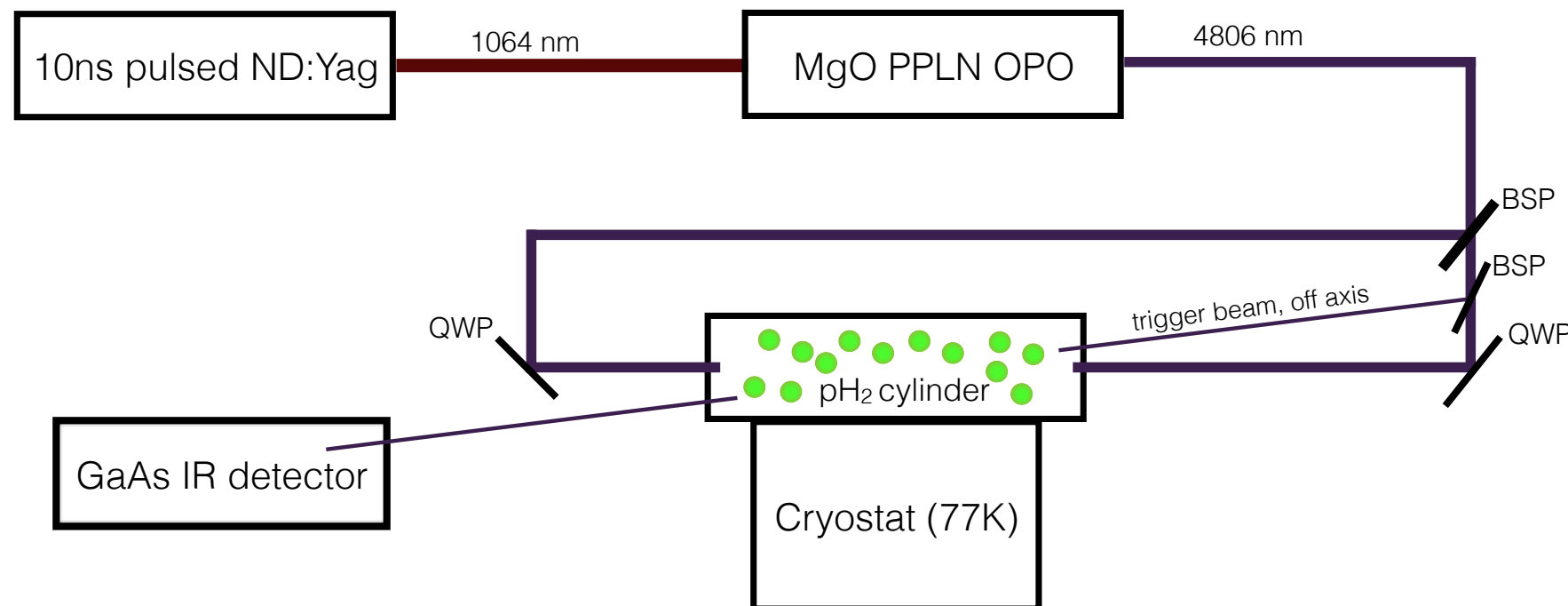
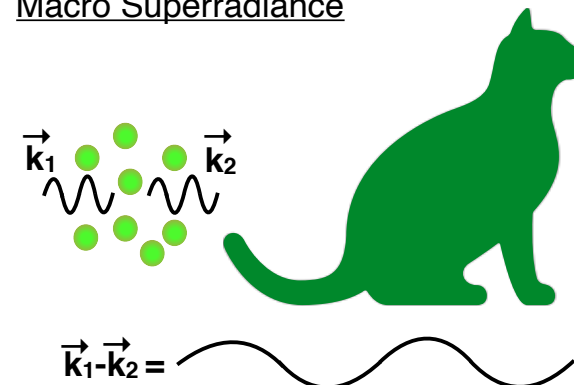
- Commercially available lasers have the pulse power necessary to excite \sim mg of parahydrogen to full coherence.
- Current record is $r_1 \sim 0.068$.

Macro Coherence at Queen's University

Dicke Superradiance



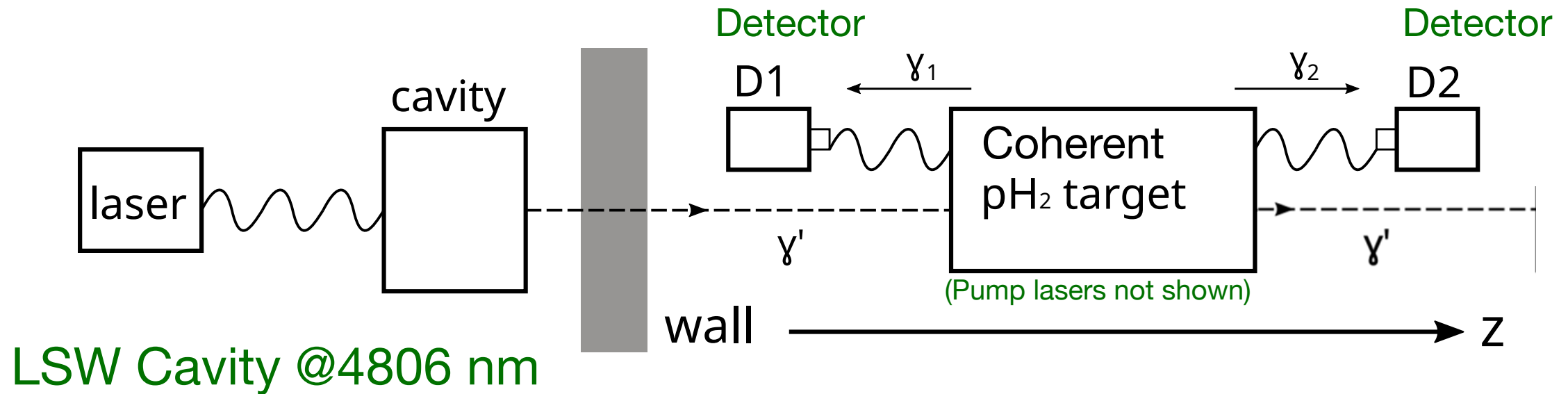
Macro Superradiance



One technical challenge is generating enough 10 ns laser pulse power
—looking into new methods for simplifying 1064 \rightarrow 4806 nm conversion.

Modified search for dark photons:

Use a macro-coherent sample of parahydrogen as a target for a light-shining-through-wall laser.

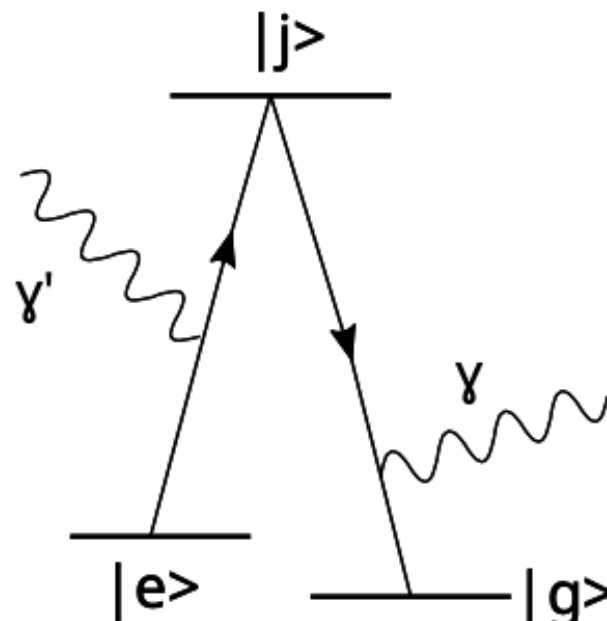


1. Excite hydrogen to coherent state with back-to-back lasers.
2. Run cavity-amplified light-through-wall laser at same frequency.
3. Look for deexcitation of pH₂ during 10 ns coherence window.
4. Calibrate coherence / response of pH₂ with cavity laser off.

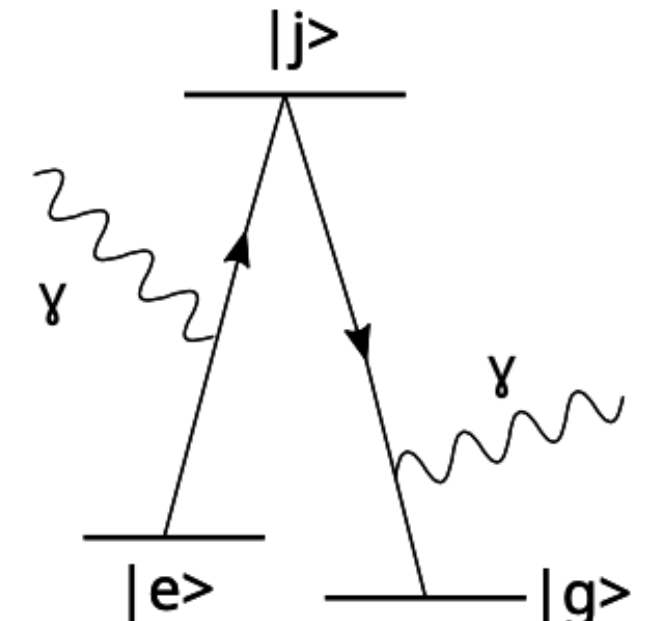
The transitions for multi-photon emission, in the Standard Model and with a dark photon.

$$H_I = -\mathbf{d} \cdot (\tilde{E}_1 + \tilde{E}_2 + \chi \tilde{E}')$$

electric dipole
term from E'

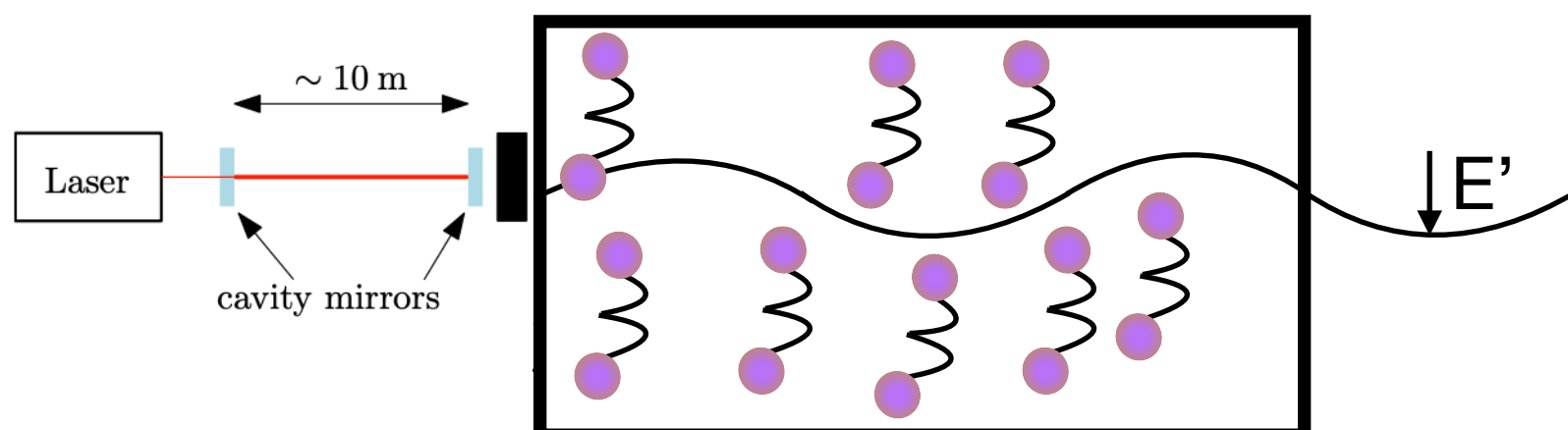


$$(a) |e\rangle \rightarrow |g\rangle + \gamma' + \gamma$$

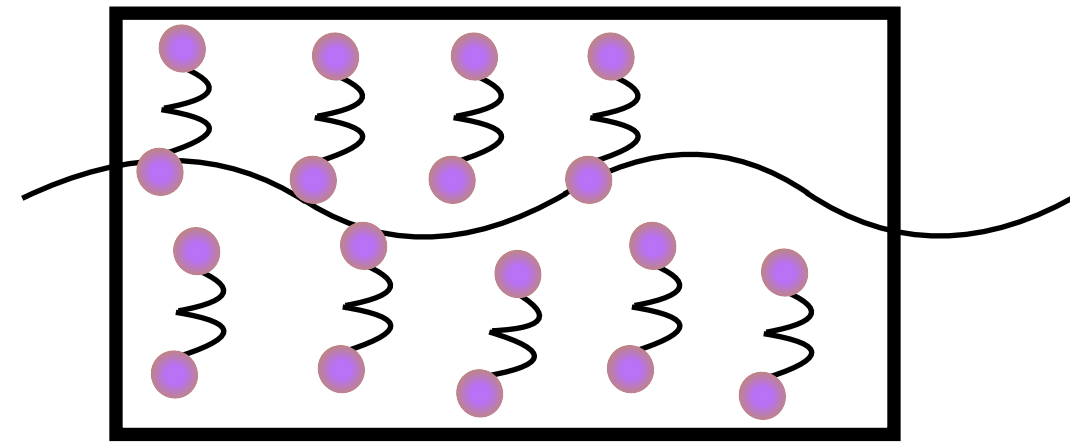
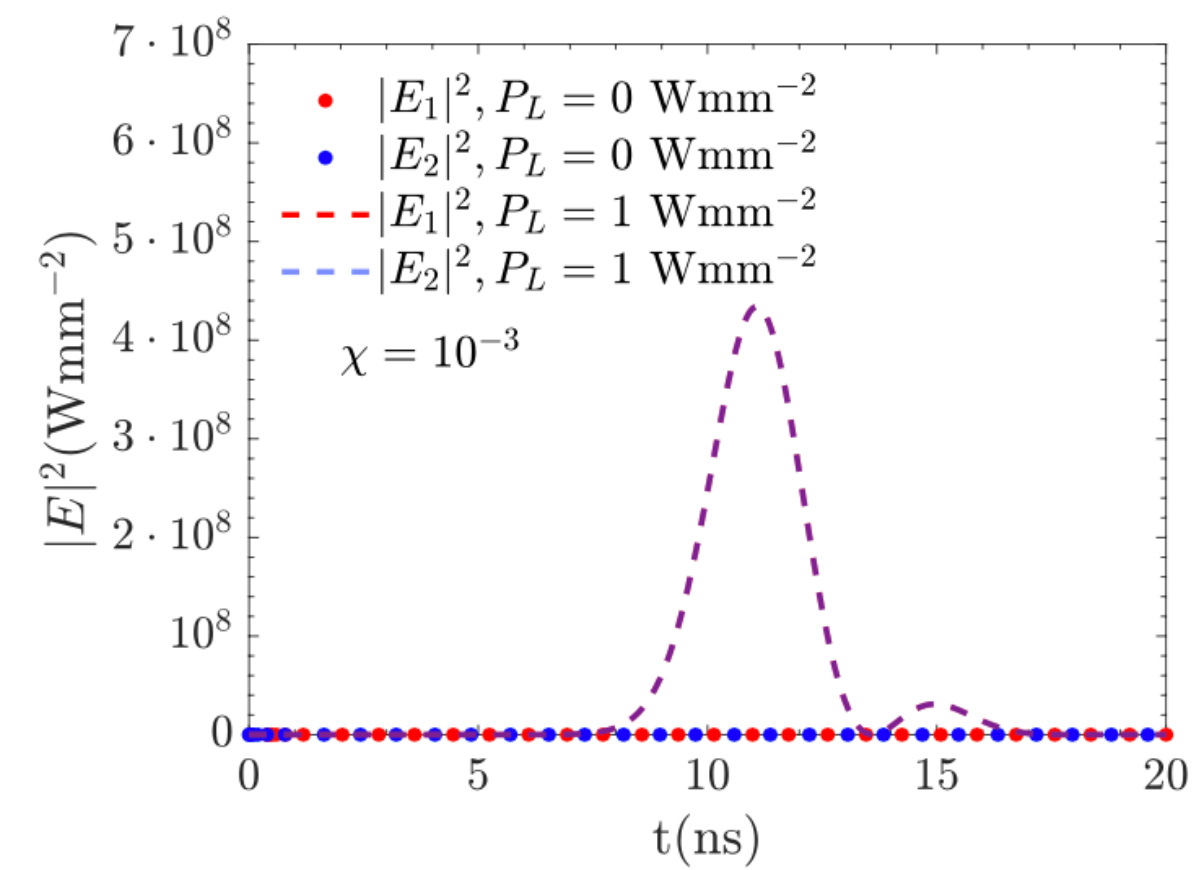
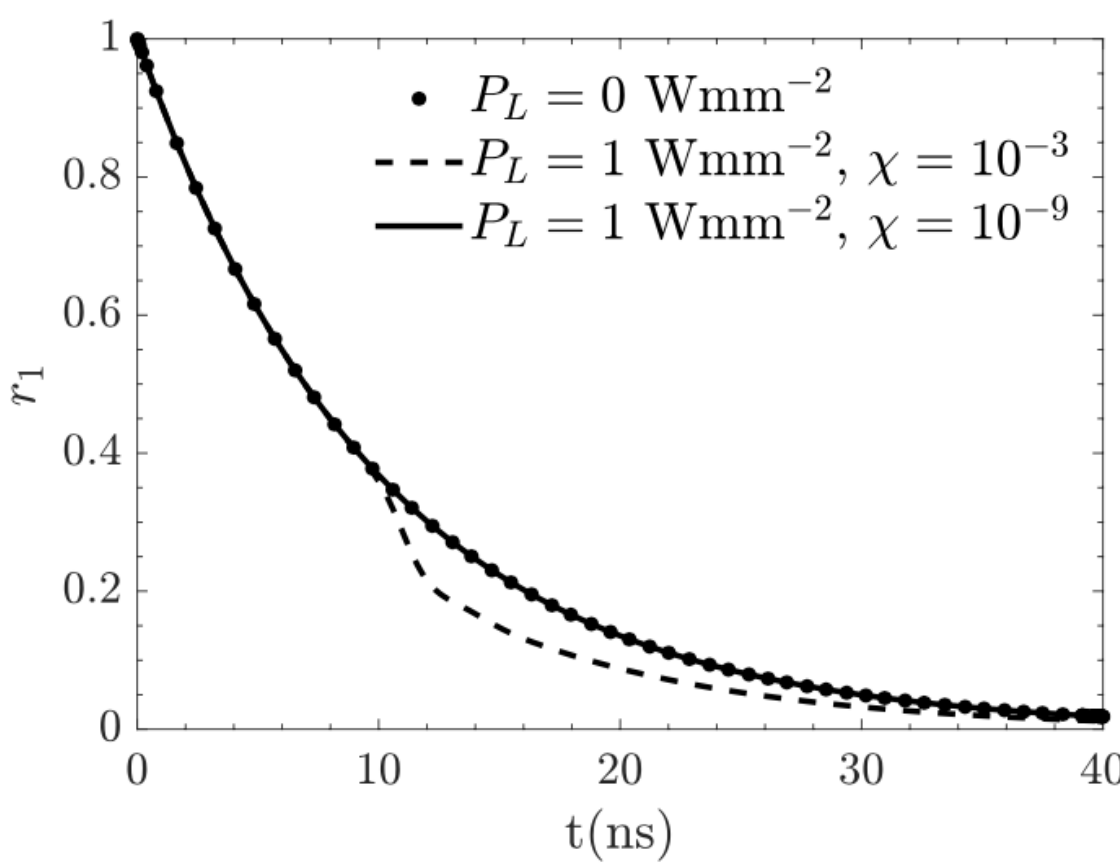


$$(b) |e\rangle \rightarrow |g\rangle + \gamma + \gamma$$

The gain over traditional light-shining-through-wall regeneration cavity is that the dark photon field acts as a trigger laser for two photon emission.



$$\Gamma = \frac{1}{8\pi} |a_{eg}|^2 |\rho_{ge}|^2 N^2 \omega_1^3 |E'|^2$$



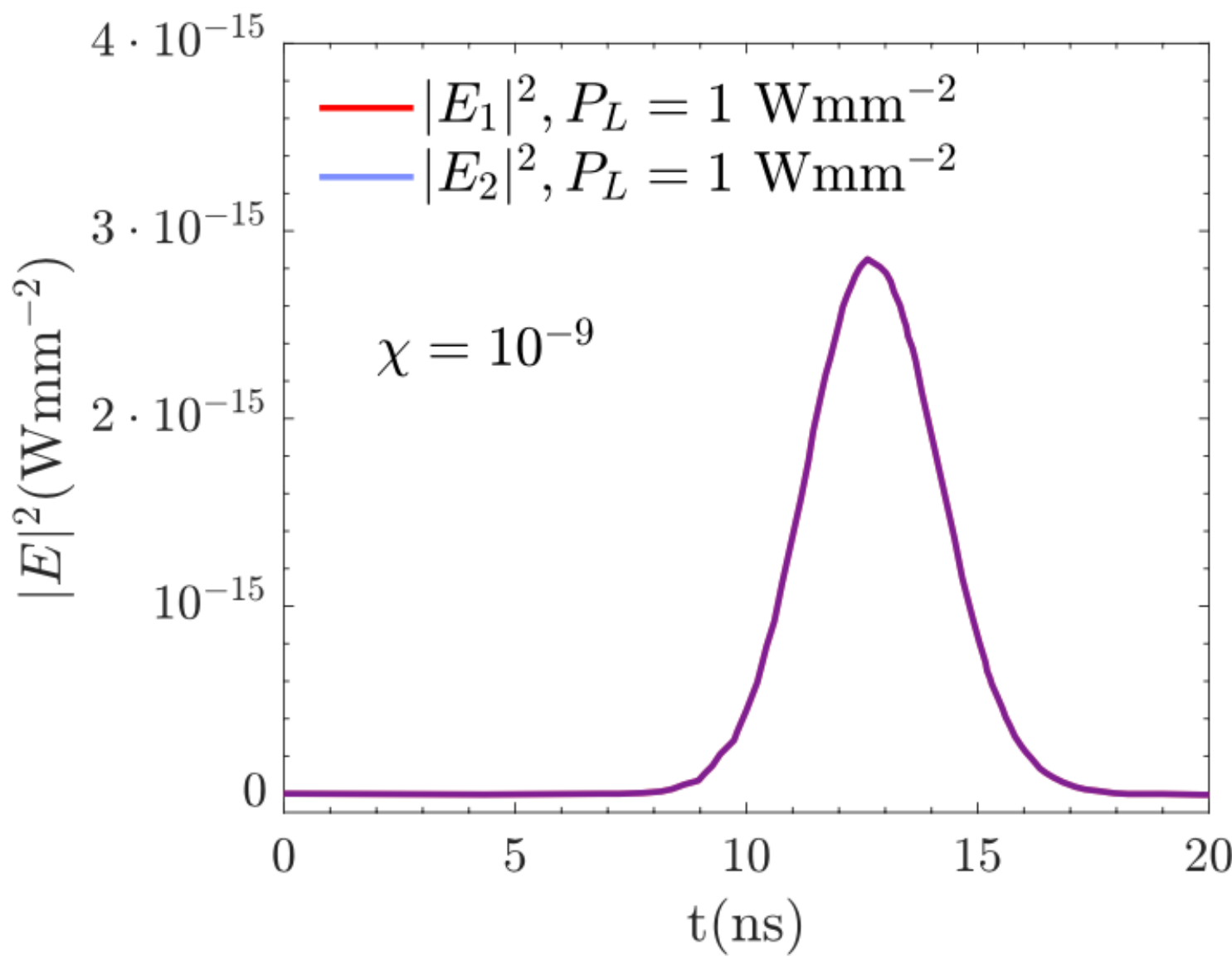
Maxwell's equations with the E1xE1 transition Hamiltonian are integrated over the experimental volume to determine the power emitted in photons from the sample, start from $r_1 = 1$.

E' , E_1 , E_2

$$(\partial_t - \partial_z)E_1 = \frac{i\omega n}{2} \left[\left(\frac{a_{ee} + a_{gg}}{2} + \frac{a_{ee} - a_{gg}}{2}r_3 \right) E_1 + a_{eg}(r_1 - ir_2)(E_2^* + \chi\eta E'^*) \right],$$

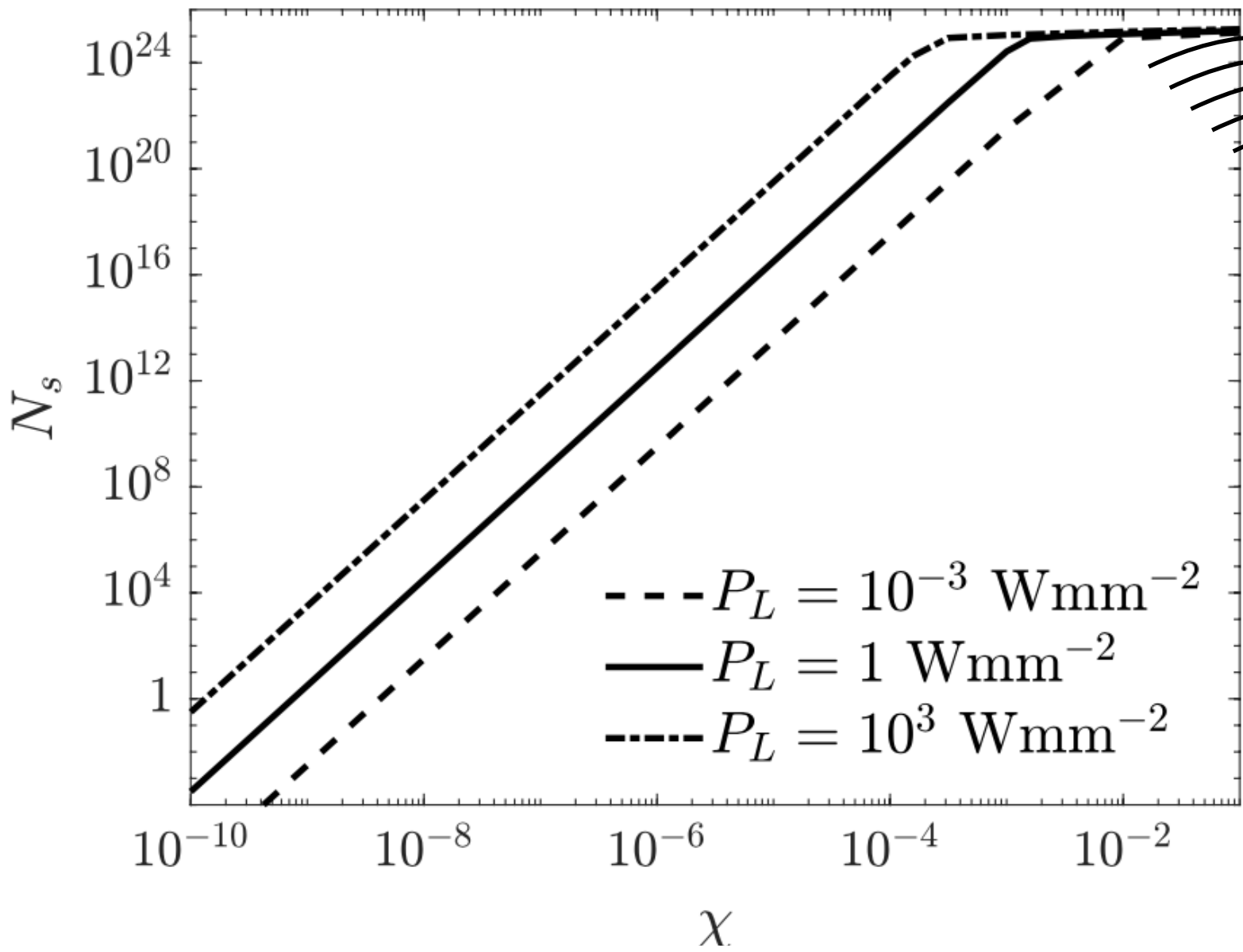
$$(\partial_t + \partial_z)E_2 = \frac{i\omega n}{2} \left[\left(\frac{a_{ee} + a_{gg}}{2} + \frac{a_{ee} - a_{gg}}{2}r_3 \right) (E_2 + \chi\eta E') + a_{eg}(r_1 - ir_2)E_1^* \right],$$

$$(\partial_t + \partial_z)E' = \frac{i\omega n}{2} \left[\left(\frac{a_{ee} + a_{gg}}{2} + \frac{a_{ee} - a_{gg}}{2}r_3 \right) (2\chi^2\eta E' + \chi E_2) + a_{eg}(r_1 - ir_2)\chi\eta E_1^* \right]$$



Using a cavity laser comparable to ALPS I, and a pH₂ macro coherence setup similar to a lower power test run [Hiraki et al. 2018], ~10 signal photons for N_{rep} = 1000, m_{A'} = 0.1 meV, χ = 10⁻⁹.

Dark Photon Generating Cavity	Superradiant Parahydrogen Target
Cavity Length $l = 50$ cm	Sample Length $L = 30$ cm
Cavity Reflections $N_{\text{pass}} = 2 \times 10^4$	pH ₂ Density $n = 10^{21} \text{ cm}^{-3}$
Cavity Laser Freq. $\omega' = 0.26$ eV	Pump Laser Freq. $\omega_1 = 0.26$ eV
Cavity Laser Power $P_L = 1 \text{ W mm}^{-2}$	Pump Laser Power $\approx 10^9 \text{ W mm}^{-2}$
—	pH ₂ Sample Area $A = 1 \text{ cm}^2$

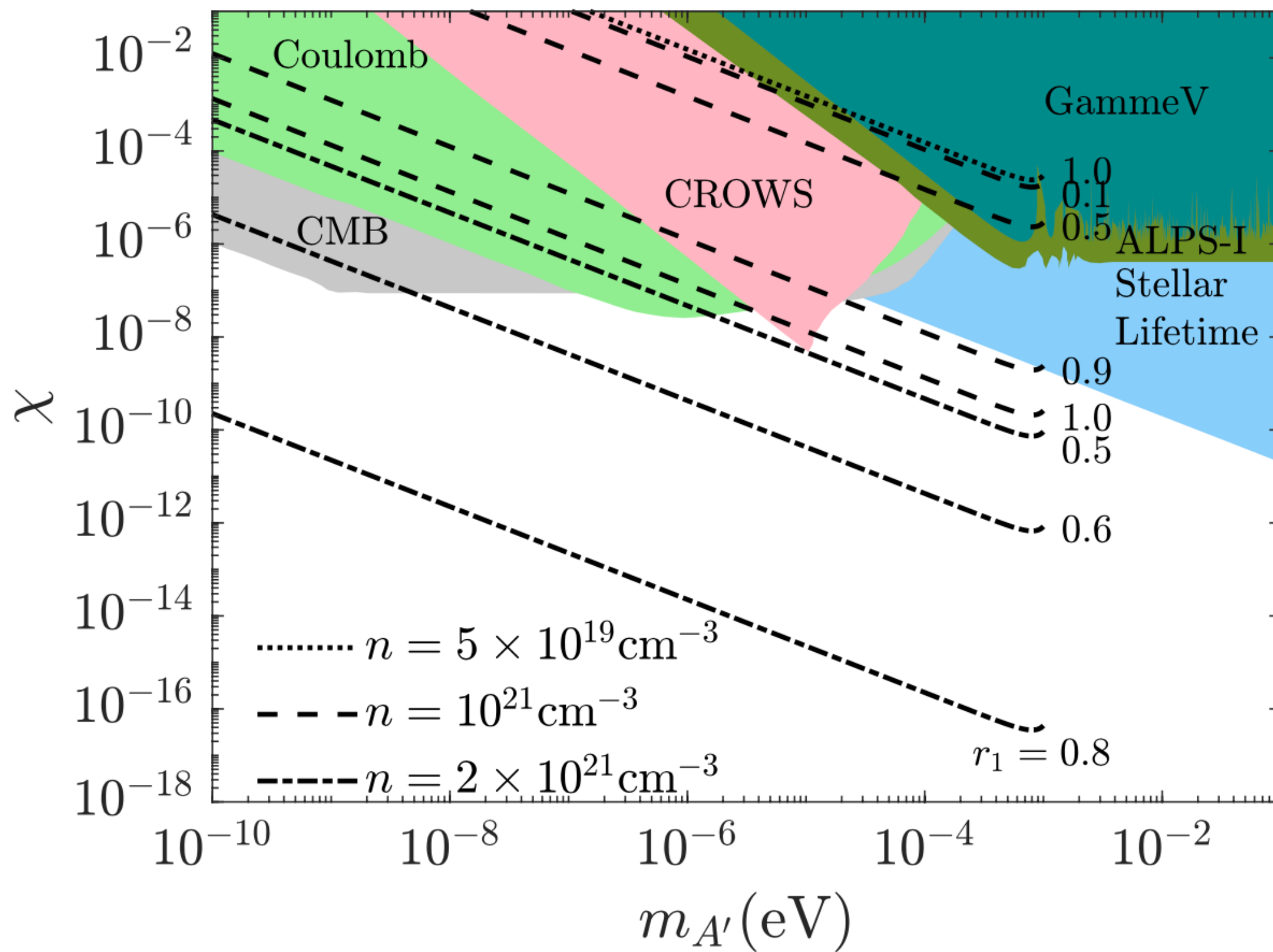


$$N_s \propto P_L N_{\text{rep}} \chi^4 (N_{\text{pass}} + 1) \sin^2 \left(\frac{m_{A'}^2}{4\omega} l \right)$$

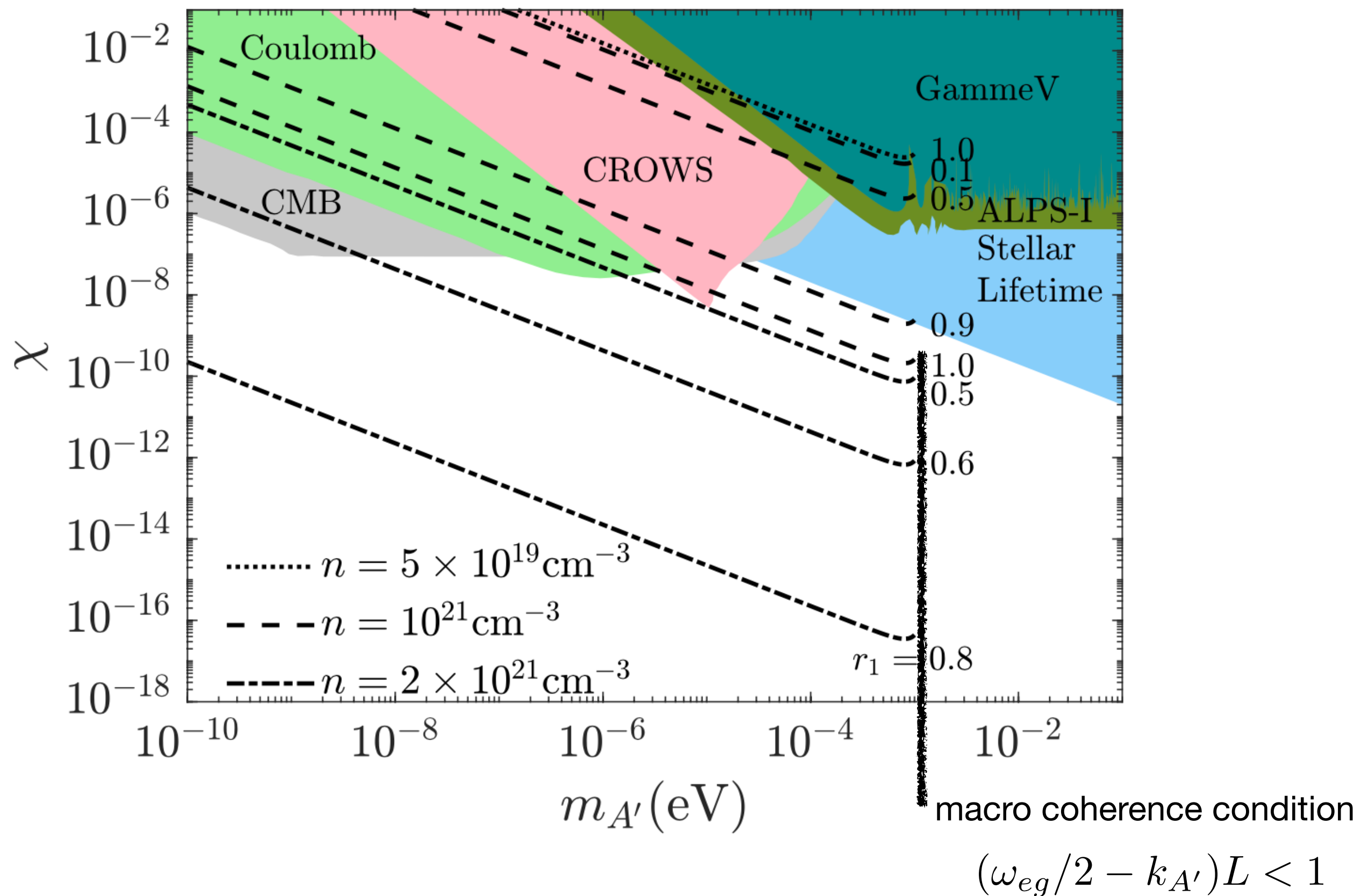
Signal photons scale the mixing parameter (until every atom is de-excited.)

Dark Photon Generating Cavity	Superradiant Parahydrogen Target
Cavity Length $l = 50 \text{ cm}$	Sample Length $L = 30 \text{ cm}$
Cavity Reflections $N_{\text{pass}} = 2 \times 10^4$	pH ₂ Density $n = 10^{21} \text{ cm}^{-3}$
Cavity Laser Freq. $\omega' = 0.26 \text{ eV}$	Pump Laser Freq. $\omega_1 = 0.26 \text{ eV}$
Cavity Laser Power $P_L = 1 \text{ W mm}^{-2}$	Pump Laser Power $\approx 10^9 \text{ W mm}^{-2}$
—	pH ₂ Sample Area $A = 1 \text{ cm}^2$

There is improved reach as the number density of pH_2 increases.



There is improved reach as the number density of pH₂ increases.



The extremely nonlinear sensitivity scaling with n (also L, t) can be understood quantitatively

$$\begin{aligned} (\partial_t - \partial_z) E_1 &= \frac{i\omega n}{2} \left[\left(\frac{a_{ee} + a_{gg}}{2} + \frac{a_{ee} - a_{gg}}{2} r_3 \right) E_1 + a_{eg}(r_1 - ir_2)(E_2^* + \chi\eta E'^*) \right], \\ (\partial_t + \partial_z) E_2 &= \frac{i\omega n}{2} \left[\left(\frac{a_{ee} + a_{gg}}{2} + \frac{a_{ee} - a_{gg}}{2} r_3 \right) (E_2 + \chi\eta E') + a_{eg}(r_1 - ir_2) E_1^* \right], \\ (\partial_t + \partial_z) E' &= \frac{i\omega n}{2} \left[\left(\frac{a_{ee} + a_{gg}}{2} + \frac{a_{ee} - a_{gg}}{2} r_3 \right) (2\chi^2\eta E' + \chi E_2) + a_{eg}(r_1 - ir_2)\chi\eta E_1^* \right] \end{aligned}$$

condense
field equations,
drop z, r₂, fix r₁

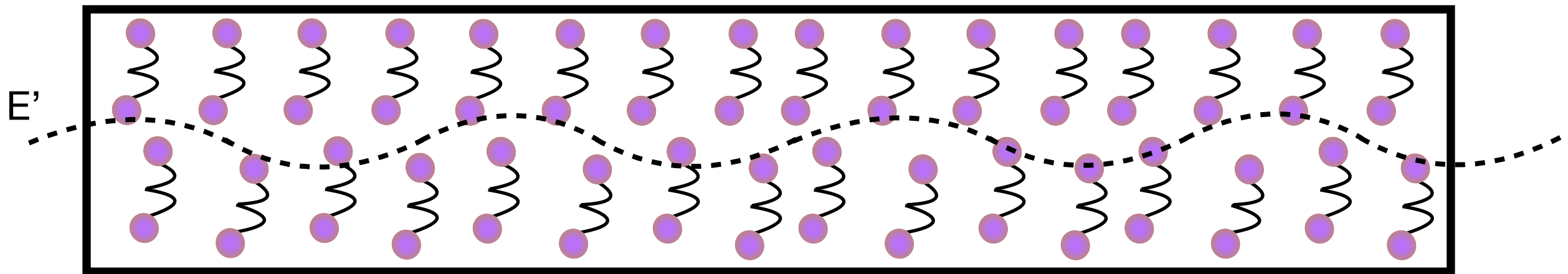
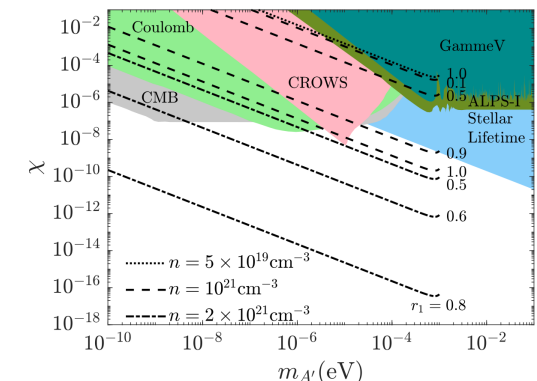
$$(\partial_t^2 - \partial_z^2) E_1 - n^2 \Omega_r^2 E_1 = 0$$

$$E_1 \propto e^{n\Omega_r t}$$

$$\Omega_r \propto \omega a_{eg} r_1$$

->Exponential dependence on n, t, r₁

and qualitatively



The extremely nonlinear sensitivity scaling with n (also L, t) can be understood quantitatively

$$\begin{aligned} (\partial_t - \partial_z) E_1 &= \frac{i\omega n}{2} \left[\left(\frac{a_{ee} + a_{gg}}{2} + \frac{a_{ee} - a_{gg}}{2} r_3 \right) E_1 + a_{eg}(r_1 - ir_2)(E_2^* + \chi\eta E'^*) \right], \\ (\partial_t + \partial_z) E_2 &= \frac{i\omega n}{2} \left[\left(\frac{a_{ee} + a_{gg}}{2} + \frac{a_{ee} - a_{gg}}{2} r_3 \right) (E_2 + \chi\eta E') + a_{eg}(r_1 - ir_2) E_1^* \right], \\ (\partial_t + \partial_z) E' &= \frac{i\omega n}{2} \left[\left(\frac{a_{ee} + a_{gg}}{2} + \frac{a_{ee} - a_{gg}}{2} r_3 \right) (2\chi^2\eta E' + \chi E_2) + a_{eg}(r_1 - ir_2)\chi\eta E_1^* \right] \end{aligned}$$

condense
field equations,
drop z, r₂, fix r₁



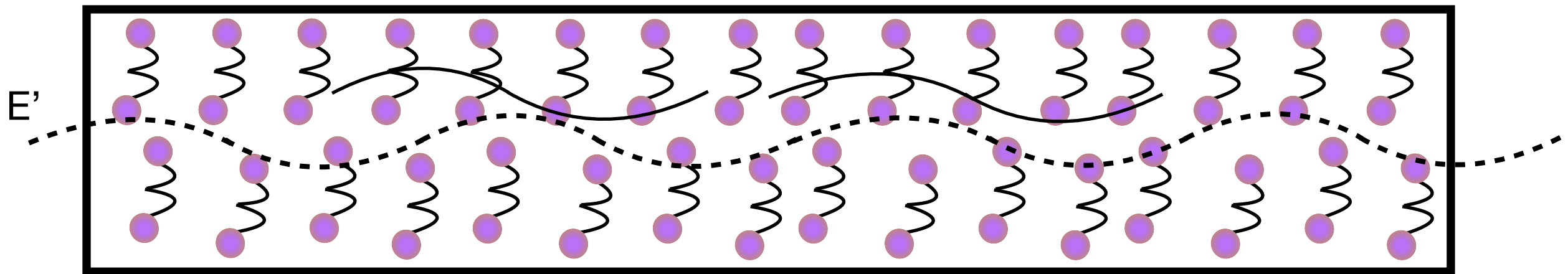
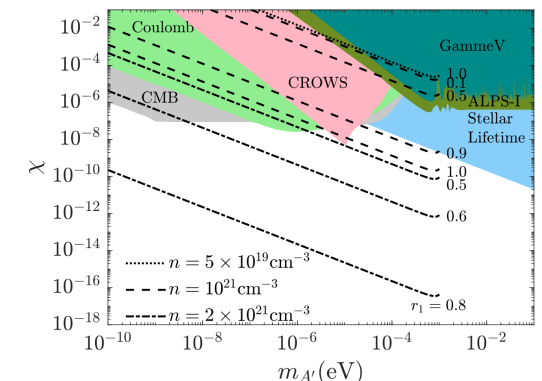
$$(\partial_t^2 - \partial_z^2) E_1 - n^2 \Omega_r^2 E_1 = 0$$

$$E_1 \propto e^{n\Omega_r t}$$

$$\Omega_r \propto \omega a_{eg} r_1$$

->Exponential dependence on n, t, r₁

and qualitatively



The extremely nonlinear sensitivity scaling with n (also L, t) can be understood quantitatively

$$\begin{aligned} (\partial_t - \partial_z) E_1 &= \frac{i\omega n}{2} \left[\left(\frac{a_{ee} + a_{gg}}{2} + \frac{a_{ee} - a_{gg}}{2} r_3 \right) E_1 + a_{eg}(r_1 - ir_2)(E_2^* + \chi\eta E'^*) \right], \\ (\partial_t + \partial_z) E_2 &= \frac{i\omega n}{2} \left[\left(\frac{a_{ee} + a_{gg}}{2} + \frac{a_{ee} - a_{gg}}{2} r_3 \right) (E_2 + \chi\eta E') + a_{eg}(r_1 - ir_2) E_1^* \right], \\ (\partial_t + \partial_z) E' &= \frac{i\omega n}{2} \left[\left(\frac{a_{ee} + a_{gg}}{2} + \frac{a_{ee} - a_{gg}}{2} r_3 \right) (2\chi^2\eta E' + \chi E_2) + a_{eg}(r_1 - ir_2)\chi\eta E_1^* \right] \end{aligned}$$

condense
field equations,
drop z, r₂, fix r₁



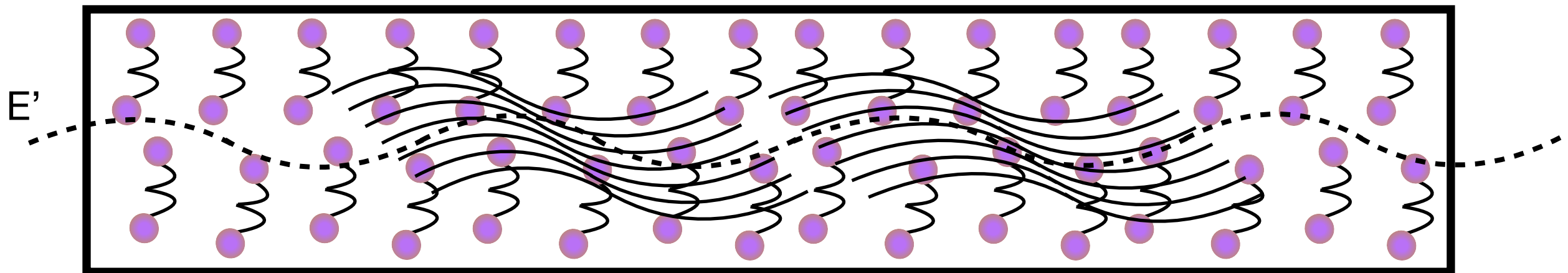
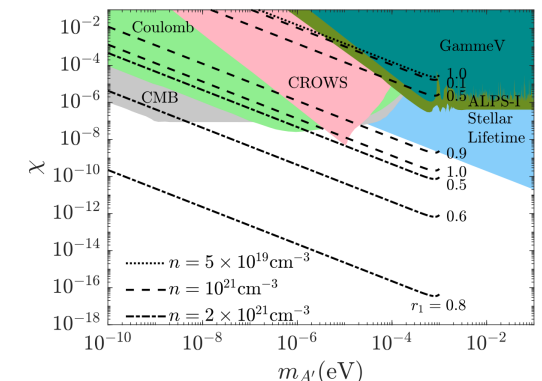
$$(\partial_t^2 - \partial_z^2) E_1 - n^2 \Omega_r^2 E_1 = 0$$

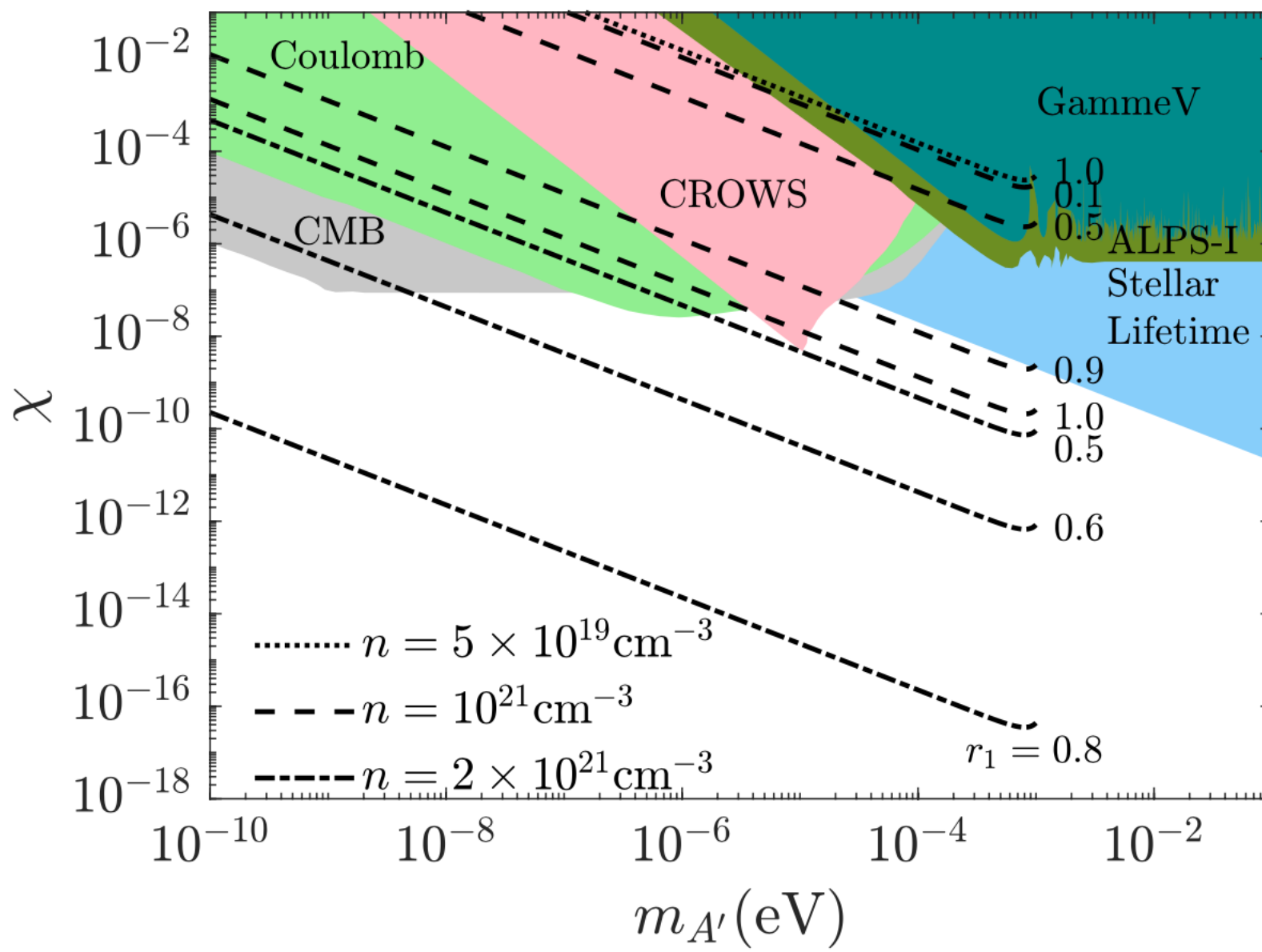
$$E_1 \propto e^{n\Omega_r t}$$

$$\Omega_r \propto \omega a_{eg} r_1$$

->Exponential dependence on n, t, r₁

and qualitatively





- Macro superradiance in parahydrogen can be used to look for weakly coupled fields
- Need to develop $r_1 \sim 1$ in a pH₂ sample, recent progress towards this goal

